

Environmental Science Processes & Impacts

Accepted Manuscript



This is an *Accepted Manuscript*, which has been through the Royal Society of Chemistry peer review process and has been accepted for publication.

Accepted Manuscripts are published online shortly after acceptance, before technical editing, formatting and proof reading. Using this free service, authors can make their results available to the community, in citable form, before we publish the edited article. We will replace this *Accepted Manuscript* with the edited and formatted *Advance Article* as soon as it is available.

You can find more information about *Accepted Manuscripts* in the [Information for Authors](#).

Please note that technical editing may introduce minor changes to the text and/or graphics, which may alter content. The journal's standard [Terms & Conditions](#) and the [Ethical guidelines](#) still apply. In no event shall the Royal Society of Chemistry be held responsible for any errors or omissions in this *Accepted Manuscript* or any consequences arising from the use of any information it contains.

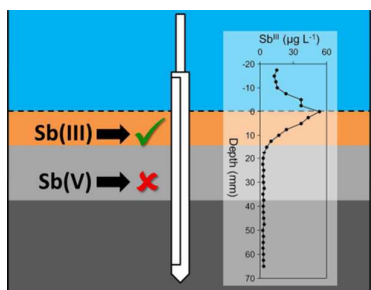


rsc.li/process-impacts

Environmental Impact Statement:

Antimony is a priority environmental contaminant, with the primary source being the mining and processing of antimony ore for industrial applications. Despite this, very little research on the behaviour and fate of antimony in the environment has been reported. To properly understand the processes controlling the movement of antimony through the environment, there is a need for tools to accurately measure the speciation of antimony, not just the total concentration. Here we report an *in situ*, passive sampling tool capable of measuring antimony speciation in surface waters and sediment porewaters. The application of this tool to investigating antimony speciation in the environment will provide new insights into the complex processes controlling its behaviour and fate.

1
2
3
4
5
6
7
8
9
10
11
12
13
14
15
16
17
18
19
20
21
22
23
24
25
26
27
28
29
30
31
32
33
34
35
36
37
38
39
40
41
42
43
44
45
46
47
48
49
50
51
52
53
54
55
56
57
58
59
60



A new *in situ* sampling method enables the selective measurement of Sb(III) in surface waters and sediment porewaters

1
2
3 1 *In situ* speciation of dissolved inorganic antimony in
4
5
6
7 2 surface waters and sediment porewaters: development
8
9
10
11 3 of a thiol-based diffusive gradients in thin films
12
13
14
15 4 technique for Sb^{III}
16
17
18
19 5
20
21
22 6
23

24 7 *William W. Bennett**, Maja Arsic, David T. Welsh and Peter R. Teasdale
25
26 8

27
28
29 9 Environmental Futures Research Institute, Griffith School of Environment, Griffith University, QLD
30
31 10 4215, Australia
32
33 11

34
35
36 12 *Corresponding Author: w.bennett@griffith.edu.au
37
38 13
39
40 14
41
42
43 15
44
45 16
46
47
48 17
49
50 18
51
52 19
53
54
55 20
56
57 21
58
59
60

Abstract

Antimony is a priority environmental contaminant typically present as either the trivalent (Sb^{III}) or the pentavalent (Sb^{V}) oxidation state in aquatic systems. Both the toxicity and mobility of antimony are affected by its speciation, and thus the accurate measurement of antimony speciation is essential for investigating the behaviour of this contaminant in aquatic systems. Here we present a diffusive gradients in thin films (DGT) technique, which utilises a binding layer containing a thiol-based adsorbent (3-mercaptopropyl functionalised silica gel), for the selective measurement of Sb^{III} in surface waters and sediment porewaters. We also evaluated the Metsorb DGT technique, which has been previously reported to accurately measure Sb^{V} , for its ability to accumulate Sb^{III} and thus allow the measurement of total inorganic antimony. Both the mercapto-silica and Metsorb DGT techniques showed a high affinity for Sb^{III} , with uptake efficiencies $>97\%$. Elution efficiencies of $86.9 \pm 2.6\%$ and $88.1 \pm 1.2\%$ were obtained for mercapto-silica and Metsorb, respectively, with $1 \text{ mol L}^{-1} \text{ H}_2\text{O}_2$ in $1 \text{ mol L}^{-1} \text{ NaOH}$. The accumulation of Sb^{III} by these DGT techniques was linear with time ($R^2 > 0.99$) and unaffected by pH (4.07 – 8.05), ionic strength ($0.001 \text{ mol L}^{-1} - 1.0 \text{ mol L}^{-1} \text{ NaCl}$), bicarbonate ($1 \text{ mmol L}^{-1} - 15 \text{ mmol L}^{-1}$), and an artificial seawater matrix (pH 8.34; salinity 34.8). Finally, the mercapto-silica DGT technique was applied to measure porewater concentrations of Sb^{III} and As^{III} in a contaminated freshwater sediment at high resolution.

1
2 47 **Introduction**

3
4 48 Antimony is a metalloid widely exploited for industrial applications, with global mine production in
5
6 49 2013 estimated at 159,000 metric tons.¹ The extensive industrial use of antimony has resulted in it
7
8
9 50 being listed as a priority pollutant by the United States Environmental Protection Agency.² Antimony
10
11 51 is primarily used in flame retardants, lead alloys for lead-acid batteries, and the production of glass,
12
13
14 52 ceramics, and plastics.¹ There have also been numerous reports of severe antimony contamination
15
16 53 surrounding mining and processing facilities, and at shooting ranges (see Filella *et al.*³ and Wilson *et*
17
18 54 *al.*⁴ for comprehensive reviews on antimony occurrence in the environment). Ultimately, inorganic
19
20
21 55 contaminants like antimony are transported to aquatic systems, where they often accumulate in
22
23 56 sediments and are subject to complex biogeochemical processes that determine their environmental
24
25
26 57 behaviour and fate. The study of antimony biogeochemistry is complicated by the fact that it exists in
27
28 58 different oxidation states; typically neutral $\text{Sb}(\text{OH})_3$ (Sb^{III}) or oxyanionic $\text{Sb}(\text{OH})_6^-$ (Sb^{V}), which can
29
30 59 impact both its affinity for various solid-phases and its toxicity to biota.⁵

31
32 60
33
34
35 61 The most reliable way to determine antimony speciation in natural waters is by on-site or *in situ*
36
37 62 separation of the species of interest. On-site approaches are limited to solid phase extraction (SPE) of
38
39
40 63 the sample, typically with SPE cartridges through which the sample is passed.⁶ Such methods have the
41
42 64 advantage of avoiding sample preservation, storage, and transport, and can be done relatively quickly
43
44
45 65 and inexpensively. Unfortunately, the methods that are available are not suitable for marine waters and
46
47 66 require volumes of sample (typically millilitres) not often obtainable when extracting sediment
48
49 67 porewater.⁶ Passive *in situ* sampling methods for antimony speciation could provide the same benefits
50
51
52 68 as on-site methods, with the additional advantage of integrating concentrations over the deployment
53
54 69 time of the sampling device, thereby providing a more representative measurement of antimony
55
56 70 concentrations in dynamic systems.⁷

57
58
59 71
60

1
2 72 Diffusive gradients in thin films (DGT) is an *in situ*, passive sampling technique that provides a time-
3
4 73 weighted average analyte concentration in surface and interstitial waters (see Zhang and Davison⁸ for a
5
6 74 recent review on the application of DGT for measurements in water, sediment and soils).^{9, 10} Solutes
7
8
9 75 diffuse through a diffusive layer of known thickness, typically a polyacrylamide hydrogel overlain by a
10
11 76 protective membrane, and are immobilised within a binding layer (often hydrogel-based) that contains
12
13
14 77 a binding agent with high affinity for the analyte of interest. The analyte concentration in the bulk
15
16 78 solution is calculated from the mass of analyte accumulated by the binding layer (determined after
17
18 79 elution and analysis of the analyte), the deployment time, the area of sampler exposed to the bulk
19
20
21 80 solution, the thickness of the diffusive layer, and the diffusion coefficient of the analyte in the diffusive
22
23 81 layer.¹⁰
24
25

26 82
27
28 83 Numerous binding agents have been used in DGT to permit the measurement of a wide variety of
29
30 84 analytes, including, for example: cationic trace metals,¹¹ oxyanionic metalloids,^{12, 13} sulfide,¹⁴
31
32
33 85 phosphate,^{15, 16} and ammonium.¹⁷ Additionally, the application of selective binding agents that only
34
35 86 accumulate a specific analyte oxidation state, have expanded the DGT technique to allow the *in situ*
36
37 87 measurement of chemical speciation. Recently, Fan *et al.*¹⁸ described the application of a 3-
38
39 88 mercaptopropyl functionalised silica-based DGT technique for measuring Sb^{III} in wastewater and
40
41
42 89 freshwater, although this method was not tested in seawater and required a complicated elution
43
44 90 procedure. Panther *et al.*¹³ described a Metsorb DGT technique for measuring Sb^V in natural waters,
45
46
47 91 although the ability of this technique to measure Sb^{III} was not tested. Bennett *et al.*¹⁹ described the use
48
49 92 of a binding layer containing 3-mercaptopropyl functionalised silica gel that selectively accumulated
50
51 93 As^{III} in the presence of As^V. When combined with a DGT technique for measuring total inorganic
52
53
54 94 arsenic, such as that described by Panther *et al.*²⁰ or Bennett *et al.*,²¹ this approach allowed the
55
56 95 quantification of As^{III} and As^V in surface waters and sediment porewaters.²²
57
58
59 96
60

1
2 97 Here we present a diffusive gradients in thin films (DGT) technique for the selective *in situ*
3
4 98 measurement of Sb^{III} in fresh and marine surface waters and sediment porewaters. The method utilizes
5
6
7 99 a thiol-based binding layer (3-mercaptopropyl functionalized silica gel immobilized in a
8
9 100 polyacrylamide gel matrix) with high selectivity for Sb^{III} over Sb^V. The existing Metsorb DGT
10
11 101 technique that was previously evaluated for measuring Sb^V,¹³ was also tested for its ability to
12
13
14 102 accurately measure Sb^{III}, which would allow this technique to be used to measure total inorganic
15
16 103 antimony. The mercapto-silica and Metsorb DGT methods were tested at a range of pH, ionic strength,
17
18
19 104 bicarbonate concentration, and in artificial seawater. Finally, the new mercapto-silica DGT method was
20
21 105 applied to determining high-resolution porewater profiles of Sb^{III} and As^{III} in a contaminated
22
23 106 freshwater sediment.
24
25
26 107
27

28 108 **Experimental**

29
30 109 **Reagents, materials and solutions.** All plasticware was washed in 5-10% HNO₃ or HCl and then
31
32
33 110 thoroughly rinsed in deionized water (18.2 MΩcm⁻¹; Millipore) before use. All reagents were analytical
34
35 111 reagent grade or better. Stock solutions (100 mg L⁻¹) of antimonite (Sb^{III}) and antimonate (Sb^V) were
36
37 112 prepared by dissolution of potassium antimony(III) tartrate and potassium hexahydroxoantimonate(V),
38
39
40 113 respectively, in deionized water. Stock solutions were stored at 4°C and diluted immediately before
41
42 114 use. DGT sampler housings were purchased from DGT Research Ltd (<http://www.dgtresearch.com>). 3-
43
44
45 115 mercaptopropyl functionalised silica gel (SiliaMetS Thiol) was purchased from Silicycle (Quebec,
46
47 116 Canada), and Metsorb HMRP (50 μm powder) was obtained from Graver Technologies (Delaware,
48
49 117 United States of America).
50
51

52 118
53
54 119 **Antimony analysis.** Antimony (m/z 121) was measured by inductively coupled plasma – mass
55
56 120 spectrometry (ICP-MS; Agilent 7900). The instrument was equipped with an octopole
57
58
59 121 collision/reaction cell, which was operated in helium collision mode to reduce potential polyatomic
60

1
2 122 interferences. All solutions for analysis were prepared in 2% (v/v) ultrapure HNO₃ (sub-boiling
3
4 123 distilled). External calibration solutions and quality control solutions were prepared from separate
5
6 124 commercially available standard solutions (High Purity Standards). A certified reference material
7
8
9 125 (Riverine Water, SLRS-5; National Research Council Canada) was analysed in each analytical run and
10
11 126 had an average recovery of 102.1 ± 6.0 % (n = 9). The stability of inorganic antimony species in the
12
13
14 127 experimental solutions was monitored using a solid phase extraction (SPE) procedure followed by ICP-
15
16 128 MS analysis, as described previously,⁶ Speciation changes were negligible over the experimental
17
18
19 129 durations used in this study. Samples taken for speciation analysis were processed immediately, to
20
21 130 avoid possible speciation changes due to storage.

22
23 131
24
25
26 132 **DGT samplers.** DGT samplers with binding layers containing either 3-mercaptopropyl functionalized
27
28 133 silica gel (mercapto-silica) or Metsorb were prepared as described previously.^{19, 21} The diffusive layers
29
30 134 of the samplers consisted of a polyacrylamide hydrogel, prepared as described previously,^{19, 21} and a
31
32
33 135 protective 0.45 µm pore-size cellulose nitrate (Merck Millipore Ltd.) or polysulfone (Pall Corp.) filter
34
35 136 membrane, with a total thickness of 0.088 ± 0.04 cm. Samplers were stored in sealed polyethylene bags
36
37
38 137 at 4°C prior to use. Following retrieval of DGT samplers from deployment solutions they were
39
40 138 thoroughly rinsed in deionised water and stored at 4°C prior to elution. DGT binding gels were eluted
41
42 139 in 1 mL of 1 mol L⁻¹ H₂O₂ / 1 mol L⁻¹ NaOH for at least 24 hours, before being diluted 20-fold in 2%
43
44
45 140 HNO₃ for ICP-MS analysis, except where stated otherwise.

46
47 141
48
49 142 **Uptake and elution.** Mercapto-silica and Metsorb binding gel discs were exposed in triplicate to
50
51 143 known volumes of 100 µg L⁻¹ Sb^{III} (pH 6, 0.01 mol L⁻¹ NaCl) for at least 12 hours. Samples of the
52
53
54 144 solution before and after exposure of the binding gel discs were collected for ICP-MS analysis to
55
56 145 determine the mass of antimony accumulated by the binding gels. Elution of antimony from the binding
57
58
59 146 gels was tested by exposing them to 1 mL of one of the following solutions for at least 24 h: 0.1 mol L⁻¹
60

1
2 147 ¹ KIO₃ / 1 mol L⁻¹ HNO₃ / 1 mol L⁻¹ HCl; or 1 mol L⁻¹ H₂O₂ / 1 mol L⁻¹ NaOH. Eluents were diluted
3
4 148 and analysed by ICP-MS to determine the efficiency of elution procedures.
5
6

7 149
8
9 150 **Accumulation over time.** To determine if the accumulation of Sb^{III} by Mercapto-silica and Metsorb
10
11 151 DGT samplers was linear, three sets of triplicate samplers were exposed to a well-stirred solution
12
13 containing 100 µg L⁻¹ Sb^{III} in 0.01 mol L⁻¹ NaCl (buffered at pH 7.79 ± 0.05 with 5.0 x 10⁻⁴ mol L⁻¹
14 152 NaHCO₃) for 10, 18, and 26 hours. A similar experiment was done to determine if Sb^V was
15
16 153 accumulated by mercapto-silica DGT, where a single set of triplicate samplers was exposed to a well-
17
18 154 stirred solution of 100 µg L⁻¹ Sb^V in 0.01 mol L⁻¹ NaCl (buffered at pH 7.90 ± 0.02 with 5.0 x 10⁻⁴ mol
19
20 L⁻¹ NaHCO₃) for 26 hours. The average temperature of the experimental solutions was 24.8 ± 0.4°C.
21 155
22
23 156 Samples of the solution were taken at the beginning of the experiment, and each time DGT samplers
24
25 157 were removed, for ICP-MS analysis of total antimony and for antimony speciation analysis by SPE-
26
27 ICP-MS.
28 158
29
30 159
31
32

33 160
34
35 161 **Effect of pH, ionic strength, bicarbonate concentration, and artificial seawater.** The performance
36
37 162 of mercapto-silica and Metsorb DGT were assessed for measuring Sb^{III} over a range of pH, ionic
38
39 strengths, bicarbonate concentrations, and in artificial seawater. DGT samplers of each type were
40 163 deployed in triplicate in well-stirred solutions containing 100 µg L⁻¹ Sb^{III} for 24 – 26 hours (exact time
41
42 164 recorded). Solutions of different pH were prepared in 0.01 mol L⁻¹ NaCl through the addition of HCl
43
44 165 (for pH < 6) or by buffering with 5.0 x 10⁻⁴ mol L⁻¹ NaHCO₃ (for pH > 7). Solutions of different ionic
45
46 166 strength were prepared with NaCl at 0.001, 0.01, 0.1, and 1.0 mol L⁻¹ (buffered at pH 7.82 ± 0.12 with
47
48 167 5.0 x 10⁻⁴ mol L⁻¹ NaHCO₃). Solutions of different bicarbonate concentration were prepared in 0.01
49
50 168 mol L⁻¹ NaCl with NaHCO₃ at 0.001, 0.005, 0.01 and 0.015 mol L⁻¹. Due to the buffering of solution
51
52 169 pH by NaHCO₃, the pH of each solution was slightly different: pH 8.20 ± 0.03 for 0.001 mol L⁻¹
53
54 170 NaHCO₃; pH 8.65 ± 0.22 for 0.005 mol L⁻¹ NaHCO₃; pH 8.81 ± 0.18 for 0.010 mol L⁻¹ NaHCO₃; and
55
56 171
57
58
59
60

1
2 172 pH 8.79 ± 0.18 for $0.015 \text{ mol L}^{-1} \text{ NaHCO}_3$. Artificial seawater was prepared as described by Grasshoff
3
4 173 *et al.*,²³ and had a pH of 8.34 ± 0.01 and a salinity of 34.8.
5
6

7 174
8
9 175 **Capacity.** The linear accumulation capacity of mercapto-silica DGT and Metsorb DGT samplers was
10
11 176 determined by exposing ten samplers of each type to a well-stirred solution of $22 \text{ mg L}^{-1} \text{ Sb}^{\text{III}}$ and
12
13
14 177 removing one sampler of each type every 30 minutes. The mass accumulated by each sampler was
15
16 178 compared to the theoretical mass calculated from the diffusion coefficient of Sb^{III} , the deployment time,
17
18 179 the area of sampler exposed to solution and the diffusive layer thickness (as per the DGT equation).¹⁰
19
20
21 180 Deviation of the measured mass from the theoretical mass indicates that the linear accumulation
22
23 181 capacity has been exceeded, and the sampler is no longer accumulating Sb^{III} quantitatively.
24
25

26 182
27
28 183 **High-resolution, porewater measurements of Sb^{III} and As^{III} with mercapto-silica DGT.** Sediment
29
30 184 was collected from an antimony and arsenic contaminated wetland in Urunga, New South Wales,
31
32
33 185 Australia ($30^{\circ}30'12.4''\text{S } 153^{\circ}00'46.1''\text{E}$), and transported to the laboratory. The sediment was sieved to
34
35 186 $< 1 \text{ mm}$ and homogenised, before being placed into a large Perspex mesocosm and allowed to stabilise
36
37
38 187 for at least one month in a constant temperature room at $21 \pm 0.2^{\circ}\text{C}$. The overlying water of the
39
40 188 mesocosm was constantly sparged with air to ensure oxic conditions. A DGT sediment sampler
41
42 189 containing a mercapto-silica binding layer for the selective measurement of Sb^{III} and As^{III} was prepared
43
44 190 with a diffusive layer consisting of a 0.08 cm -thick bisacrylamide-crosslinked polyacrylamide hydrogel
45
46
47 191 covered with a 0.01 cm -thick $0.45 \mu\text{m}$ -poresize cellulose nitrate filter membrane. The sampler was
48
49 192 deoxygenated in $0.01 \text{ mol L}^{-1} \text{ NaNO}_3$ sparged with nitrogen gas for at least 2 hours prior to
50
51
52 193 deployment. The sampler was deployed in the sediment for 24 hours, after which time it was removed,
53
54 194 thoroughly rinsed with deionised water, and stored at 4°C prior to processing and analysis. The
55
56 195 mercapto-silica binding gel was cut from the DGT sampler and washed for at least 1 hour in 50 mL of
57
58
59 196 deionised water to remove unbound solutes, before being laterally sliced at 2.5 mm intervals and each
60

1
2 197 slice eluted in 0.5 mL of 0.01 mol L⁻¹ KIO₃ / 1 mol L⁻¹ HNO₃ / 1 mol L⁻¹ HCl for 24 hours. A sub-
3
4 198 sample of each eluent was diluted 20-fold in 2% HNO₃ prior to analysis by ICP-MS. A blank DGT
5
6
7 199 sampler was processed in the same way to determine the limit of detection (3σ).
8

9 200 10 11 201 **Results and Discussion**

12 202 **Uptake and elution.** Uptake efficiencies of Sb^{III} by mercapto-silica and Metsorb binding gels were
13
14 202 99.5% and 97.9%, respectively, which provided initial verification that these binding gels had a high
15
16 203 affinity for Sb^{III} and were suitable for further testing. Elution of Sb^{III} from Metsorb was done using 1
17
18 204 mol L⁻¹ H₂O₂ / 1 mol L⁻¹ NaOH, as previously described for the elution of Sb^V from Metsorb binding
19
20
21 205 gels,¹³ and resulted in an Sb^{III} elution efficiency of 88.1 ± 1.2%. The elution of Sb^{III} from mercapto-
22
23 206 silica binding gels was tested with 0.1 mol L⁻¹ KIO₃ / 1 mol L⁻¹ HNO₃ / 1 mol L⁻¹ HCl (which is similar
24
25 207 to the procedure previously reported for the elution of As^{III} from the same binding layer¹⁹); and 1 mol
26
27
28 208 L⁻¹ H₂O₂ / 1 mol L⁻¹ NaOH, which resulted in elution efficiencies of 62.6 ± 1.4% and 86.9 ± 2.6%,
29
30 209 respectively. The comparatively high elution efficiency obtained with 1 mol L⁻¹ H₂O₂ / 1 mol L⁻¹
31
32 210 NaOH may be due to the oxidation of the thiol functional groups on the mercapto-silica under these
33
34
35 211 conditions. These elution procedures are much simpler than that reported by Fan *et al.*¹⁸ for the same
36
37 212 binding gel, which required microwave-assisted extraction in concentrated HNO₃, HCl, and HF.
38
39 213 Subsequent elution of Sb^{III} from DGT binding layers in this study was done with 1 mol L⁻¹ H₂O₂ / 1
40
41
42 214 mol L⁻¹ NaOH, except where otherwise stated. Depending on the analytical equipment being used for
43
44 215 the quantification of antimony in the eluent solutions, it may be more appropriate to use the 0.1 mol L⁻¹
45
46 216 KIO₃ / 1 mol L⁻¹ HNO₃ / 1 mol L⁻¹ HCl eluent solution to minimise the dilution required before
47
48 217 analysis. The Agilent 7900 ICP-MS used in this study was tuned to have a robust plasma (i.e. CeO:Ce
49
50 218 < 0.2%) that was capable of analysing 1 mol L⁻¹ H₂O₂ / 1 mol L⁻¹ NaOH eluent solutions after only a 10
51
52 219 or 20-fold dilution, with negligible ionisation suppression due to high sodium ion concentrations.
53
54 220
55
56 221
57
58
59
60

1
2 222 **Accumulation over time.** The accumulation of Sb^{III} by mercapto-silica DGT and Metsorb DGT was
3
4 223 tested by deploying samplers of each type in triplicate for 10, 18, and 26 hours. Unfortunately, the
5
6 224 instability of Sb^{III} in laboratory solutions prevented longer deployment times. Linear regression of the
7
8
9 225 mass of Sb^{III} accumulated by the samplers over time confirmed that the uptake process was linear, with
10
11 226 R² values of 0.999 and 0.991 for mercapto-silica DGT and Metsorb DGT, respectively (Figure S1).
12
13
14 227 Effective diffusion coefficients were calculated as described previously¹⁹ from the slope of the
15
16 228 regression line, the ICP-MS-measured concentration of antimony in the deployment solution, the
17
18 229 thickness of the diffusive layer, and the area of the sampler exposed to the solution. The effective
19
20
21 230 diffusion coefficients of Sb^{III} estimated from the mercapto-silica DGT and Metsorb DGT data were
22
23 231 $9.42 \times 10^{-6} \text{ cm}^2 \text{ s}^{-1}$ and $8.23 \times 10^{-6} \text{ cm}^2 \text{ s}^{-1}$ at 25°C, respectively. These values are similar to the
24
25
26 232 diffusion coefficient previously reported for As^{III} ($9.04 \times 10^{-6} \text{ cm}^2 \text{ s}^{-1}$), which is a similar neutral
27
28 233 oxyanion.¹⁹ The diffusion coefficient of Sb^{III} reported by Fan *et al.*¹⁸ is only 32% of the value
29
30 234 determined in this study. This discrepancy is unlikely to be due to the difference in binding layer
31
32
33 235 materials, as suggested by Fan *et al.*,¹⁸ because the polyethersulfone membrane used in their study has
34
35 236 been used as a component of DGT diffusive layers previously without retarding diffusion to such a
36
37
38 237 large extent.²⁴ To ensure accurate results, we recommend that laboratories independently determine
39
40 238 diffusion coefficients with their specific DGT configuration.

41
42 239
43
44 240 The accumulation of Sb^V by mercapto-silica DGT was also tested over 26 hours, and was found to be
45
46
47 241 negligible (mass of Sb^V accumulated was ~2% of the mass of Sb^{III} accumulated over the same time)
48
49 242 (Figure S1). This provides initial verification that mercapto-silica DGT can be used to selectively
50
51
52 243 measure Sb^{III} in the presence of Sb^V, thus providing speciation information. Furthermore, previous
53
54 244 research by Panther *et al.*¹³ has demonstrated that Metsorb DGT quantitatively measures Sb^V, which in
55
56 245 association with this work demonstrating its ability to measure Sb^{III}, confirms that Metsorb DGT can be
57
58
59 246 used to measure total inorganic antimony (Sb^{III} + Sb^V). The simultaneous application of both mercapto-
60

silica DGT, for selectively measuring Sb^{III} ; and Metsorb DGT, for measuring both Sb^{III} and Sb^{V} , will allow the determination of inorganic antimony speciation in natural waters. Such an approach to *in situ* speciation using DGT has been described in detail previously for inorganic arsenic.^{19, 25}

Effect of pH, ionic strength, bicarbonate concentration, and artificial seawater. The performance of mercapto-silica DGT and Metsorb DGT under various solution conditions is summarised in Table 1. Both mercapto-silica DGT and Metsorb DGT show acceptable performance under all tested conditions, indicating that these techniques can be deployed in a variety of natural water types with confidence. Importantly, this is the first time that a thiol-based DGT technique has been tested for its ability to measure Sb^{III} in a seawater matrix and in the high concentrations of bicarbonate often found in sediment porewaters due to the microbial metabolism of organic matter. Previous work by Panther *et al.*²⁶ demonstrated the importance of considering bicarbonate as an interference, particularly for the measurement of oxyanionic species by DGT techniques with metal oxide-based binding gels.

Table 1. Effect of pH, ionic strength, bicarbonate concentration, and artificial seawater on the measurement of Sb^{III} by mercapto-silica DGT (C_{MSIL}) and Metsorb DGT (C_{MET}). The concentration of antimony in solution (C_{SOLN}) was measured by ICP-MS.

<i>Parameter</i>		$C_{\text{MSIL}}:C_{\text{SOLN}}$	$C_{\text{MET}}:C_{\text{SOLN}}$
pH	4.07	0.99 ± 0.10	1.17 ± 0.08
	6.15	1.06 ± 0.04	1.09 ± 0.05
	8.05	0.98 ± 0.04	1.06 ± 0.04
Art. seawater (pH 8.35)		0.93 ± 0.13	0.99 ± 0.03
Ionic strength	0.001 mol L ⁻¹	1.05 ± 0.03	1.14 ± 0.05
	0.01 mol L ⁻¹	1.00 ± 0.07	1.10 ± 0.05

(as NaCl)	0.1 mol L ⁻¹	0.98 ± 0.01	1.14 ± 0.03
	1.0 mol L ⁻¹	0.95 ± 0.01	1.05 ± 0.09
	1 mmol L ⁻¹	1.08 ± 0.06	1.09 ± 0.08
[HCO ₃ ⁻]	5 mmol L ⁻¹	1.04 ± 0.08	1.14 ± 0.11
	10 mmol L ⁻¹	1.15 ± 0.02	1.04 ± 0.10
	15 mmol L ⁻¹	1.12 ± 0.05	1.03 ± 0.05

As the purpose of the mercapto-silica DGT technique is to selectively measure Sb^{III}, unlike Metsorb DGT that is designed to measure total inorganic antimony (Sb^{III} + Sb^V), the effect of pH on the accumulation of Sb^V by mercapto-silica DGT was tested to ensure that this technique remained selective for Sb^{III} over a range of environmentally relevant pH (Figure 1).

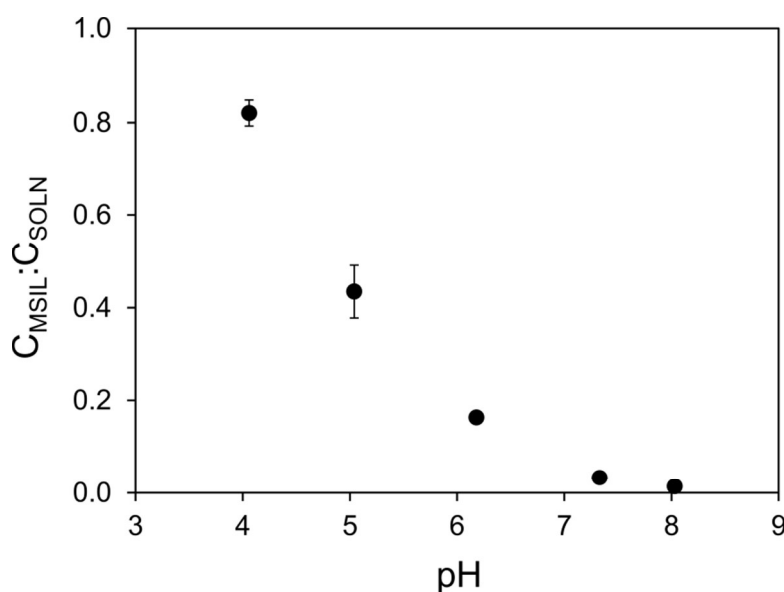


Figure 1. Effect of solution pH on the accumulation of Sb^V by mercapto-silica DGT as shown by the ratio of the concentration measured by mercapto-silica DGT (C_{MSIL}) to the concentration measured in solution by ICP-MS (C_{SOLN}). Error bars represent ± 1 standard deviation from the mean (n=3).

1
2 275 The solution pH had a strong effect on the accumulation of Sb^{V} by mercapto-silica DGT. At pH 4.06
3
4 276 the accumulation of Sb^{V} is close to quantitative, as indicated by a $C_{\text{MSIL}}:C_{\text{SOLN}}$ value of 0.82. The ratio
5
6
7 277 decreased at pH 5.04 to 0.43, and at pH 6.18 it was only 0.16. Above pH 7, the accumulation of Sb^{V} by
8
9 278 mercapto-silica DGT was negligible ($C_{\text{MSIL}}:C_{\text{SOLN}} < 0.03$). The most likely explanation for the
10
11 279 accumulation of Sb^{V} by mercapto-silica at lower pH is the reduction of Sb^{V} to Sb^{III} by the thiol
12
13
14 280 functional groups, a phenomena observed previously in antimonial drug compounds,²⁷ followed by
15
16 281 adsorption of Sb^{III} to the mercapto-silica. At pH 4.06, the rate of the reduction reaction appears to be
17
18
19 282 sufficiently rapid to facilitate adsorption of Sb to the mercapto-silica without the accumulation of
20
21 283 antimony at the interface of the binding and diffusive layers. As the pH increases, the rate of the
22
23 284 reduction reaction may not be sufficiently rapid to allow adsorption of the antimony as it diffuses into
24
25
26 285 the sampler, causing the concentration at the interface of the binding and diffusive layers to increase,
27
28 286 which retards further diffusion of Sb^{III} from the bulk solution and results in the accumulation departing
29
30 287 from the linear theoretical response.¹⁰ We recommend that Sb^{III} concentrations measured with the
31
32
33 288 mercapto-silica DGT technique be interpreted with caution when deployed in natural waters below pH
34
35 289 6.5, as there may be a confounding effect of Sb^{V} adsorption at lower pH. Future work should examine
36
37
38 290 if this effect is observed in natural waters at low pH to further resolve the boundaries of acceptable
39
40 291 deployment conditions for this technique.

41
42 292
43
44
45 293 **Capacity.** The capacity of mercapto-silica DGT and Metsorb DGT for Sb^{III} was tested to ensure that
46
47 294 the binding layers have sufficient reactive sites for extended deployments, or deployment at high
48
49 295 antimony concentrations (e.g. at contaminated sites). The results of these experiments (Figure S2) show
50
51
52 296 that these DGT techniques exhibit linear accumulation capacity for Sb^{III} in excess of 100 μg of Sb^{III} per
53
54 297 binding layer disc. This capacity is sufficient, for example, to allow deployment for over 30 days at an
55
56 298 Sb^{III} concentration of 100 $\mu\text{g L}^{-1}$ (25°C), although other factors such as biofilm formation may restrict
57
58
59 299 deployments to shorter durations in natural waters. This capacity is similar to that reported for As^{III}
60

1
2 300 with mercapto-silica DGT (77.5 μg), but much higher than that reported for As^{III} with Metsorb DGT
3
4 301 (8.5 μg).¹⁹ The high capacity for antimony indicates that these techniques are suitable for
5
6 302 measurements at both contaminated and uncontaminated sites, however, we recommend that DGT
7
8 303 techniques are evaluated at field-relevant concentrations and deployment times before their application
9
10
11 304 to new deployment conditions. Users of this technique should also account for the possibility of
12
13
14 305 exceeding the analyte capacity due to the adsorption of non-target solutes that are accumulated by the
15
16 306 binding layer (e.g. arsenite), particularly at contaminated sites.
17
18
19 307

20
21 308 **High-resolution, porewater measurements of Sb^{III} and As^{III} with mercapto-silica DGT.** To
22
23 309 demonstrate the capability of the newly developed mercapto-silica DGT technique, it was applied to
24
25 310 measuring co-distributions of Sb^{III} and As^{III} in a contaminated freshwater sediment (Figure 2). The
26
27
28 311 calculated DGT detection limits of Sb^{III} and As^{III} were $0.06 \mu\text{g L}^{-1}$ and $0.04 \mu\text{g L}^{-1}$, respectively, and all
29
30 312 measured concentrations were above these values. It should be noted that the pH of the overlying water
31
32
33 313 in this mesocosm was ~ 5.2 during the DGT deployment, which could result in the measurement of
34
35 314 some Sb^{V} if it were present in the system, as explained earlier (see Figure 1).
36
37
38
39
40
41
42
43
44
45
46
47
48
49
50
51
52
53
54
55
56
57
58
59
60

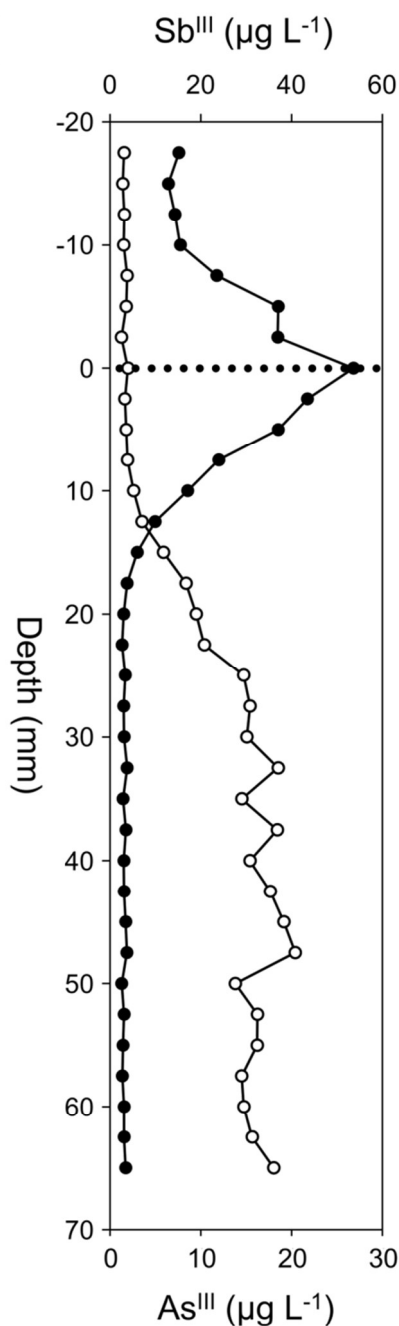


Figure 2. Porewater profile of Sb^{III} (●) and As^{III} (○) measured by mercapto-silica DGT in a contaminated freshwater wetland sediment at 2.5 mm resolution. The dotted line indicates the position of the sediment-water interface.

Sb^{III} exhibits a sharp concentration maximum at the sediment-water interface, followed by a steep concentration decrease over a depth of 20 mm. Conversely, As^{III} is present at very low concentrations

1
2 322 to 10 mm depth, after which point the concentration gradually increases and plateaus at ~30 mm depth.
3
4 323 This is the first time that such contrasting porewater concentration profiles of Sb^{III} and As^{III} have been
5
6 324 observed at the millimetre scale in aquatic sediments. The steep Sb^{III} concentration gradient across the
7
8
9 325 sediment-water interface is clearly represented by numerous data points, due to the high spatial
10
11 326 resolution possible with the DGT technique – such a concentration profile would not be obtainable with
12
13
14 327 conventional sediment core slicing and porewater extraction techniques. Furthermore, the process of
15
16 328 porewater extraction, transport and storage could result in antimony and arsenic speciation changes
17
18 329 before analysis (e.g. oxidation), thus resulting in an erroneous interpretation of the sediment chemistry
19
20
21 330 of these contaminants. In contrast, the mercapto-silica DGT technique selectively accumulates the
22
23 331 reduced oxidation states of antimony and arsenic *in situ*, and thus preserves the speciation information
24
25
26 332 at the time of sampling. The accurate measurement of different oxidation states is integral to
27
28 333 investigating the complex biogeochemical processes associated with antimony and arsenic mobilisation
29
30 334 and sequestration. Future work should systematically apply the mercapto-silica DGT technique for the
31
32
33 335 selective measurement of Sb^{III} and As^{III}, in association with the Metsorb DGT technique for measuring
34
35 336 total Sb and As, in order to further investigate the geochemical behaviour of antimony and arsenic in
36
37 337 aquatic sediments.

38
39
40 338
41
42 339 **Conclusion.** The mercapto-silica DGT method presented here provides a significant advance in the
43
44 340 speciation analysis of antimony in circumneutral natural waters. Combined with the existing Metsorb
45
46
47 341 DGT method, it is possible to individually determine both Sb^{III} and Sb^V under a wide range of
48
49 342 environmental conditions, including fresh and marine surface waters and sediment porewaters.
50
51
52 343 Furthermore, this *in situ* approach avoids many of the common issues associated with conventional *ex*
53
54 344 *situ* speciation analysis, such as speciation changes during sample collection, transport and storage.
55
56 345
57
58
59
60

1
2 346 The application of these DGT techniques to investigating the sediment biogeochemistry of antimony
3
4 347 will allow researchers to selectively measure antimony species in sediment porewaters at higher spatial
5
6
7 348 resolution than previously possible. This is particularly important in productive freshwater and coastal
8
9 349 sediments, where changes in biogeochemical zonation, and possibly antimony speciation, can occur
10
11 350 over small spatial scales. The insight gained from this approach will allow a greater understanding of
12
13
14 351 the complex biogeochemical processes that govern the mobility of antimony in aquatic systems.
15

16 352 17 18 19 353 **Acknowledgements**

20
21 354 The authors acknowledge funding provided by the Australian Research Council to W.W.B.
22
23 355 (DE140100056). The authors also thank Graver Technologies (www.gravertech.com) for the provision
24
25
26 356 of the Metsorb product used in this study.
27

28 357 29 30 358 **References**

- 31
32
33 359 1. D. E. Guberman, *2013 Minerals Yearbook*, United States Geological Survey, 2015.
- 34 360 2. USEPA, Priority Pollutant List, <http://www.epa.gov/sites/production/files/2015-09/documents/priority-pollutant-list-epa.pdf>, (accessed 14/12, 2015).
- 35 361 3. M. Filella, N. Belzile and Y.-W. Chen, *Earth-Sci. Rev.*, 2002, **57**, 125-176.
- 36 362 4. S. C. Wilson, P. V. Lockwood, P. M. Ashley and M. Tighe, *Environ. Pollut.*, 2010, **158**, 1169-1181.
- 37 363 5. M. Filella, P. A. Williams and N. Belzile, *Environ. Chem.*, 2009, **6**, 95-105.
- 38 364 6. C. Yu, Q. Cai, Z.-X. Guo, Z. Yang and S. B. Khoo, *Analyst*, 2002, **127**, 1380-1385.
- 39 365 7. B. Vrana, G. Mills, I. Allan, E. Dominiak, K. Svensson, J. Knutsson, G. Morrison and R. Greenwood, *Trends Anal. Chem.*, 2005, **24**, 845-868.
- 40 366 8. H. Zhang and W. Davison, *Environ. Chem.*, 2015, **12**, 85-101.
- 41 367 9. W. Davison and H. Zhang, *Nature*, 1994, **367**, 546-548.
- 42 368 10. H. Zhang and W. Davison, *Anal. Chem.*, 1995, **67**, 3391-3400.
- 43 369 11. O. Garmo, O. Royset, E. Steinnes and T. Flaten, *Anal. Chem.*, 2003, **75**, 3573-3580.
- 44 370 12. Q. Sun, J. Chen, H. Zhang, S. Ding, Z. Li, P. N. Williams, H. Cheng, C. Han, L. Wu and C. Zhang, *Anal. Chem.*, 2014, **86**, 3060-3067.
- 45 371 13. J. G. Panther, R. R. Stewart, P. R. Teasdale, W. W. Bennett, D. T. Welsh and H. Zhao, *Talanta*, 2013, **105**, 80-86.
- 46 372 14. P. Teasdale, S. Hayward and W. Davison, *Anal. Chem.*, 1999, **71**, 2186-2191.
- 47 373 15. J. G. Panther, P. R. Teasdale, W. W. Bennett, D. T. Welsh and H. Zhao, *Environ. Sci. Technol.*, 2010, **44**, 9419-9424.
- 48 374 16. S. Ding, D. Xu, Q. Sun, H. Yin and C. Zhang, *Environ. Sci. Technol.*, 2010, **44**, 8169-8174.

- 1
2 381 17. J. Huang, W. W. Bennett, D. T. Welsh, T. Li and P. R. Teasdale, *Anal. Chim. Acta*, 2016, **904**,
3 382 83-91.
4 383 18. H.-T. Fan, A.-J. Liu, B. Jiang, Q.-J. Wang, T. Li and C.-C. Huang, *RSC Advances*, 2016, **6**,
5 384 2624-2631.
6 385 19. W. W. Bennett, P. R. Teasdale, J. G. Panther, D. T. Welsh and D. F. Jolley, *Anal. Chem.*, 2011,
7 386 **83**, 8293-8299.
8 387 20. J. G. Panther, K. P. Stillwell, K. J. Powell and A. J. Downard, *Anal. Chim. Acta*, 2008, **622**,
9 388 133-142.
10 389 21. W. W. Bennett, P. R. Teasdale, J. G. Panther, D. T. Welsh and D. F. Jolley, *Anal. Chem.*, 2010,
11 390 **82**, 7401-7407.
12 391 22. W. W. Bennett, P. R. Teasdale, J. G. Panther, D. T. Welsh, H. Zhao and D. F. Jolley, *Environ.*
13 392 *Sci. Technol.*, 2012, **46**, 3981-3989.
14 393 23. K. Grasshoff, M. Ehrhardt, K. Kremling and L. G. Anderson, *Methods of seawater analysis*,
15 394 Wiley-VCH, 3rd edn., 1999.
16 395 24. O. A. Garmo, W. Davison and H. Zhang, *Anal. Chem.*, 2008, **80**, 9220-9225.
17 396 25. J. Gorny, L. Lesven, G. Billon, D. Dumoulin, C. Noiriel, C. Pirovano and B. Madé, *Talanta*,
18 397 2015, **144**, 890-898.
19 398 26. J. G. Panther, P. R. Teasdale, W. W. Bennett, D. T. Welsh and H. Zhao, *Anal. Chim. Acta*,
20 399 2011, **698**, 20-26.
21 400 27. C. dos Santos Ferreira, P. Silveira Martins, C. Demicheli, C. Brochu, M. Ouellette and F.
22 401 Frézard, *BioMetals*, **16**, 441-446.
23 402
24
25
26
27
28
29
30
31
32
33
34
35
36
37
38
39
40
41
42
43
44
45
46
47
48
49
50
51
52
53
54
55
56
57
58
59
60